# Third-Harmonic Generation in Ultrathin Films of MoS$_2$

Rui Wang, Hui-Chun Chien, Jatinder Kumar, Nardeep Kumar, Hsin-Ying Chiu,* and Hui Zhao*

Department of Physics and Astronomy, The University of Kansas, Lawrence, Kansas 66045, United States

ABSTRACT: We observe optical third-harmonic generation in atomically thin films of MoS$_2$ and deduce effective third-order nonlinear susceptibilities on the order of 10^{-19} m^2/V^2, which is comparable to that of commonly used semiconductors under resonant conditions. By measuring the susceptibility as a function of light wavelength, we find significant enhancements of the susceptibility by excitonic resonances. The demonstrated third-harmonic generation can be used for nonlinear optical identification of MoS$_2$ atomic layers with high contrast, better distinguishing power of multilayers, and less restrictions to substrate selections. The size of the third-order nonlinear susceptibility suggests feasibility of exploring other types of third-order nonlinear optical effects of MoS$_2$ two-dimensional crystals.

KEYWORDS: MoS$_2$, two-dimensional crystals, thin films, nonlinear optics, harmonic generation
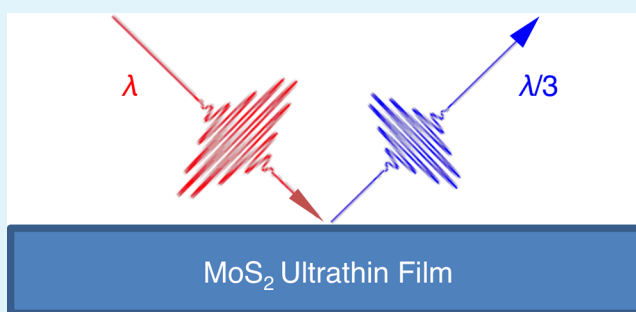
■ INTRODUCTION

Despite the remarkable progress in recent years in graphene research,[1] future applications of graphene in logic electronics are challenging due to the lack of a band gap. Although several approaches have been developed to open a sizable band gap, the mobility and the operational conditions are often compromised.[2−7] Recently, significant efforts have been directed to exploring other two-dimensional (2D) materials, such as MoS$_2$. In 2011, top-gated transistors based on ultrathin films of MoS$_2$ were demonstrated.[8] Later, integrated circuits based on monolayers[9] and bilayers[10] of MoS$_2$ for logic operations were developed. Ambipolar transport in a multilayer MoS$_2$ double-layer transistor was demonstrated,[11] showing the feasibility to develop p−n junction-based devices. Recent studies also revealed superior mechanical properties of MoS$_2$ 2D crystals, which are important for applications in 2D flexible electronics.[12−14]

Interests in exploring optoelectronic and photonics applications of MoS$_2$ 2D crystals are largely stimulated by the observation of an indirect-to-direct transition from bulk to monolayer in two photoluminescence experiments.[15,16] Bulk MoS$_2$ is an indirect semiconductor with a band gap of about 1.29 eV in the Γ valley and two dominant excitonic resonances in the K valley, called "A" and "B" excitons, with energies of 1.88 and 2.04 eV, respectively.[17] Since the "A" and "B" excitonic states are mainly from the localized d orbits on Mo atoms, they are less sensitive to the interlayer couplings, and hence are almost thickness-independent. However, the energy states in the Γ valley involve the antibounding p$_z$ orbitals in the S atoms that are sensitive to interlayer couplings.[16,18] As a result, when decreasing the thickness, the band gap in the Γ valley increases from the bulk value to about 1.9 eV in the monolayer, making monolayer MoS$_2$ a direct semiconductor. Such a direct band gap in the visible range, combined with the superior mechanical

and transport properties as well as workfunctions that are compatible with commonly used electrode materials, makes MoS$_2$ 2D crystals attractive candidates for various optoelectronic and photonic applications, as have been demonstrated in phototransistors[19,20] and heterojunction solar cells.[21]

In addition to these potential applications, MoS$_2$ 2D crystals also provide a unique platform to study 2D excitons and many-body systems. It has unusually large exciton[22] and trion[23,24] binding energies. The strong spin−orbit coupling and the lack of inversion symmetry in monolayer MoS$_2$ allow valley selective optical coupling, which can be used to explore valley and spin physics.[25−29] Furthermore, a recent theory predicted a variety of interesting magnetoelectric effects in bilayer MoS$_2$ owing to the strong coupling of spin, layer pseudospin, and valley degrees of freedom for holes in the K valley in this unique system.[30]

The interaction between light and electrons in MoS$_2$ 2D crystals includes not only linear but also higher-order nonlinear terms. The nonlinear processes can play important roles in applications involving intensive light. However, studies of nonlinear optical properties of MoS$_2$ 2D crystals, and even bulk crystals, are rare. Very recently, four groups (including us) independently observed second-harmonic generation, one important type of second-order nonlinear optical process, in ultrathin films of MoS$_2$,[31−33] WS$_2$,[34] and BN.[33] This process does not exist in bulk or even layers that are inversion-symmetric, but is strong in monolayer or few odd layers due to the symmetry broken.[31−34] So far, third-order nonlinearities of MoS$_2$ have not been studied. In contrast, several types of third-order nonlinear optical effects in graphene have been recently

studied, including saturable absorption,[35] four-wave mixing,[36] two-photon absorption,[37] coherent self phase modulation,[38] third-harmonic generation,[39,40] and optical Kerr effect.[41]

Here, we report the first study of a third-order nonlinear optical effect in ultrathin films of MoS_2. We observe third-harmonic generation (THG) and deduce effective third-order nonlinear optical susceptibilities on the order of 10^{-19} m^2/V^2. This effect can be used for nonlinear optical identification of MoS_2 atomic layers with higher contrast and higher distinguishing power of multilayer flakes, compared to linear optical microscopy. Furthermore, this technique is less restrictive on the selection of substrates. Our results suggest the feasibility of exploring other types of third-order nonlinear optical effects of this material for various photonic and optoelectronic applications.

■ EXPERIMENTAL SECTION

Atomically thin films of MoS_2 are fabricated by mechanical exfoliation[42] with an adhesive tape from natural crystals (SPI Supplies). By depositing flakes of MoS_2 on a silicon substrate with a 90 nm SiO_2 layer, we can identify large, isolated, and thin layers of MoS_2 with an optical microscope, by utilizing optical contrasts enhanced by the multilayer substrate.[43,44] We studied several flakes and observed similar results. Figure 1a shows an optical microscope
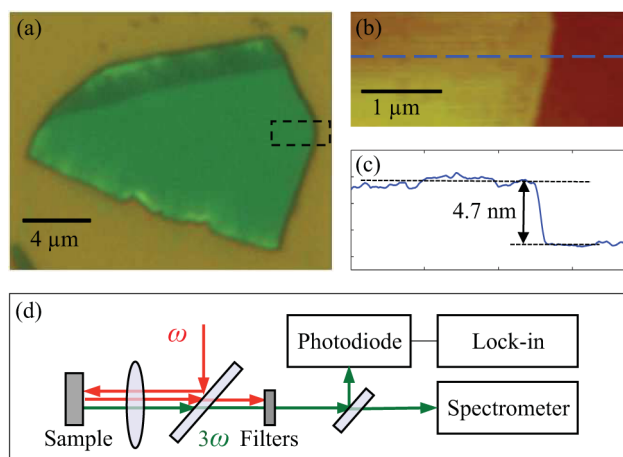
Figure 1. Sample characterization and experimental setup. (a) Optical microscopy image of a MoS_2 flake under white light illumination. (b) Atomic force microscopy image of the area indicated as the dashed box in (a). (c) A cross section of (b), as indicated by the dashed line in (b), indicates a flake thickness of 4.7 nm. This corresponds to seven atomic layers. (d) Experimental setup: a tightly focused fundamental beam (ω, red) is incident to the sample from the normal direction. The generated third harmonic (3ω, green) is detected by a spectrometer and a photodiode attached to a lock-in amplifier.

image of a relatively large and uniform flake that is taken in reflection geometry under white light illumination. To determine the number of atomic layers, we perform atomic force microscopy measurement of a region of the flake, as marked as the dashed box in Figure 1a. The result is shown in Figure 1b. According to a cross section shown in Figure 1c, the thickness of the flake is 4.7 nm. Since a monolayer of MoS_2 (one Mo layer sandwiched by two S layers) is about 0.65 nm, we conclude that this flake contains seven atomic layers.

Figure 1d shows the experimental setup to study THG. We focus a near-infrared laser pulse (ω) with a central wavelength of 1758 nm and a temporal width of about 320 fs to the sample surface by using a microscope objective lens. The pulse is obtained from an optical parametric oscillator pumped by a Ti:sapphire laser with a repetition rate of 81 MHz. The reflected third harmonic (TH, 3ω) from the

sample is collected by the same lens. A set of color filters is used to block the ω beam. A spectrometer, equipped with a thermoelectric cooled silicon charge-coupled device (CCD) camera, is used to record the TH spectra. To convert the measured CCD counts to the power of the TH radiation from the sample, we send a laser pulse with a known power and a central wavelength of 560 nm to the sample and measure the spectrum of its reflection under the same conditions. Hence, in this calibration procedure, we have included the effect of substrate reflection, the loss of all involved optics, and the sensitivity of the spectrometer.

■ RESULTS AND DISCUSSION

The inset of Figure 2 shows a spectrum of TH (green) generated by a linearly polarized ω pulse with an average power
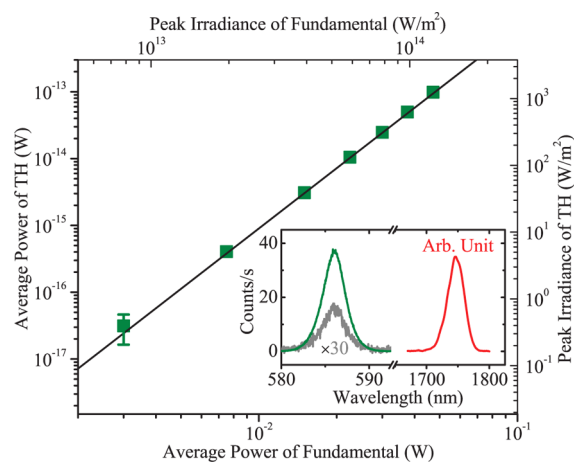
Figure 2. Average power of the third-harmonic (TH) beam (left axis) as a function of the average power of the fundamental beam (bottom axis) measured from the seven-layer MoS_2 flake. The on-axis peak irradiance of each beam is also given as the top and right axes, for convenience. Except for the first point, the error bars are smaller than the symbols. The solid line indicates a cubic dependence. The inset shows spectra of the fundamental (red, in arbitrary units), the TH from the flake (green, in CCD counts per second), and the TH from the substrate (gray, multiplied by a factor of 30 for clarity).

of 30 mW from the seven-layer MoS_2 flake shown in Figure 1a. The spectrum of the ω pulse is also plotted. The central wavelength of TH is 586 nm, which is exactly one-third of 1758 nm, the central wavelength of the ω pulse. By using a polarizer in front of the spectrometer as a polarization analyzer, we find that the TH is linearly polarized along the same direction as the ω pulse. When the laser spot is moved from the flake to bare substrate, a signal that is about 60 times weaker is detected, as shown as the gray line. This confirms that the TH is indeed generated from the MoS_2 flake.

To compare the magnitude of the third-order nonlinear optical response of MoS_2 2D crystals with other materials, we deduce an effective third-order nonlinear susceptibility, $\chi^{(3)}$, by treating the sample as a bulk medium, and solving the coupled-wave equations.[45] Since the flake thickness is much smaller than both the absorption depth and the coherence length, we can ignore the depletion of the ω beam and the phase walkoff in the THG process. These conditions greatly simplify the calculation. The TH field amplitude is related to the ω field amplitude by

$$\mathcal{E}_{3\omega} = \frac{1}{4} \frac{i3\omega}{2n_{3\omega}c} \chi^{(3)} \mathcal{E}_\omega^{3} d \qquad (1)$$

where c is the speed of light in a vacuum, d is the flake thickness, and $n_{3\omega}$ is the index of refraction at 3ω. Each field amplitude is related to its irradiance by $I_i = n_i \varepsilon_0 c \mathcal{E}_i \mathcal{E}_i^*/2$, where i stands for ω or 3ω. To relate the on-axis peak irradiance of ω, I_0, to the measured average power, $\overline{P}_\omega$, we consider that the irradiance is Gaussian in both time and space, with widths (full width at half-maxima) of τ and W, respectively. Hence,

$$\overline{P}_\omega = \frac{1}{8}\left(\frac{\pi}{\ln 2}\right)^{3/2} f \tau W^2 I_0 \qquad (2)$$

where f is the repetition rate of the laser.

To use these equations to extract the magnitude of $\chi^{(3)}$, we use values appropriate to our experiment (i.e., d = 4.7 nm, W = 3.5 μm, τ = 320 fs, λ = 1758 nm, and f = 81 MHz) and previously reported value of the index of refraction of $n_{3\omega}$ = 5.3.[44] For the index of refraction of ω, we use a value of 4.11, which is obtained from Cauchy's equation with two known values in the transparent range: 4.3 at 1064 nm[46] and 4.22 at 1240 nm.[47] We extract a value of $\chi^{(3)}$ on the order of 10^{-19} m^2/V^2. We note that the THG process is described by the real part of the complex nonlinear susceptibility only, and therefore, this value is for the real part. However, in resonant processes, the real and imaginary parts of $\chi^{(3)}$ are usually similar, such as in graphene.

On the basis of eq 1, the average power of 3ω varies as the cube of the ω power. To confirm such a dependence, we measure the TH spectra with various average powers of the ω beam. The results are summarized in the main panel of Figure 2. The solid line indicates the expected cubic dependence, which is consistent with the experimental result. In this range of the fundamental power, no sign of saturation is observed.

It is well-known that nonlinear optical responses can be enhanced if the medium has energy levels that are resonant with involved optical frequencies. The THG process can be enhanced if there are electronic states that are resonant with ω, 2ω, and/or 3ω.[45] To study the influence of the band structure of MoS$_2$ 2D crystals on its third-order nonlinearity, we repeat these measurements by tuning the central wavelength of the ω pulse, while keeping its average power a constant. The deduced magnitude of $\chi^{(3)}$ as a function of ω wavelength is shown in Figure 3. In this wavelength range, both ω and 2ω are below any interband transitions in MoS$_2$; hence, resonance enhancement can only originate from 3ω. Figure 3 shows two peaks with 3ω wavelengths of 650 and 595 nm, respectively. These wavelengths are about 20 nm shorter than the A (670 nm) and B (620 nm) exciton transitions of samples with similar thicknesses that were previously measured by absorption[48] and photoluminescence spectroscopy.[15,16] Since the wavelength difference between these two peaks (45 nm) and the width of each peak (about 20 nm) are consistent very well with the two excitonic transitions, we attribute these two peaks to the excitonic enhancement of the third-order nonlinear optical process. However, the origin of the 20 nm blue shift of these peaks with respect to the exciton resonances is unclear. It is not induced by sample heating, since the exciton transitions would shift to longer wavelength at higher temperatures.

Figure 3 also shows that, when the ω wavelength is longer than 1980 nm, no TH can be observed under the same conditions. On the basis of the signal-to-noise ratio of our detection system, the $\chi^{(3)}$ is at most 10^{-22} m^2/V^2. We note that, in this wavelength range, the 3ω is below the excitonic resonances, but still resonant with the indirect band-to-band
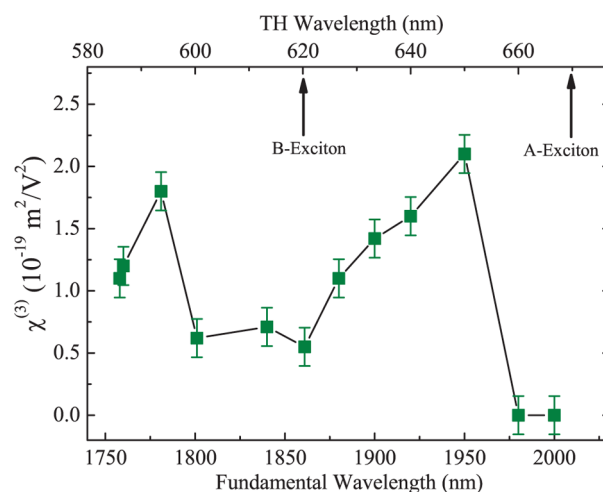
Figure 3. Measured third-order nonlinear susceptibility as a function of fundamental wavelength (bottom axis) and third-harmonic (TH) wavelength (top axis). The A and B excitonic absorption peak wavelengths for a sample with a comparable thickness are marked as vertical arrows.

transitions in MoS$_2$. Hence, the excitonic enhancement is at least 3 orders of magnitude higher than that due to the indirect band-to-band transitions.

The deduced $\chi^{(3)}$ of ultrathin films of MoS$_2$ is comparable to that of other semiconductors that are widely used in photonics and optoelectronics, such as Si, Ge, and GaAs, under resonant conditions.[45] Hence, our results illustrate potential applications of MoS$_2$ 2D crystals in third-order nonlinear optics, and may stimulate further investigations on other types of third-order nonlinear optical effects. On the other hand, the measured $\chi^{(3)}$ in MoS$_2$ is about 3 orders of magnitude smaller than that in graphene.[39] This can be attributed to the fact that, in graphene, the resonant enhancement occurs at ω, 2ω, and 3ω, whereas, in MoS$_2$, only the 3ω photons are resonant.

The observed THG can be used as an effective way to identify and determine the thickness of multilayer MoS$_2$. Previously, optical identifications of MoS$_2$ atomic layers relied on contrast enhancement of multilayer reflections, which is mainly achieved by using Si/SiO$_2$ substrates with a certain thickness of the oxide layer. This imposes constrains on substrate selections. Furthermore, even with optimal substrates, identification of multilayers with more than 10 atomic layers is rather challenging since the contrast difference is very small. The recently observed second-harmonic generation can be used to image monolayers.[31−34] However, it is less effective to study multilayers since the effect is absent in even layers, and decreases with layer number in odd layers.[31−34] The THG provides an alternative way for optical identification of MoS$_2$ atomic layers. By comparing the spectra from the seven-layer flake and from the substrate (inset of Figure 2), we obtain an intensity contrast of about $I_{\text{sample}}/I_{\text{substrate}} \approx 60$. This contrast is actually limited by the THG from the silicon substrate. When transparent substrates with much weaker THG are used, the contrast would be further increased. Since the TH intensity depends quadratically on the flake thickness or number of layers for thin films in which absorption of ω and TH is negligible (see eq 1), the TH intensity from the monolayer would be a factor of 49 times smaller than that from the seven-layer flake. Hence, the contrast for monolayer would be 60/49 $\approx$ 1.2. This is a few times higher than the optimal contrast of

the monolayer in linear optical microscopy.[43] In addition to the enhanced contrast, the THG can more easily distinguish multilayer flakes owing to the quadratic thickness dependence of the TH intensity. Furthermore, it can be used with any substrates with weak THG, in particular, transparent substrates that are preferred for optical measurements.

To illustrate the feasibility of using THG to identify MoS_2 atomic layers, we acquire a TH image of another flake with regions of different thicknesses by scanning the ω spot across the sample. Figure 4a shows an optical microscopy image of the
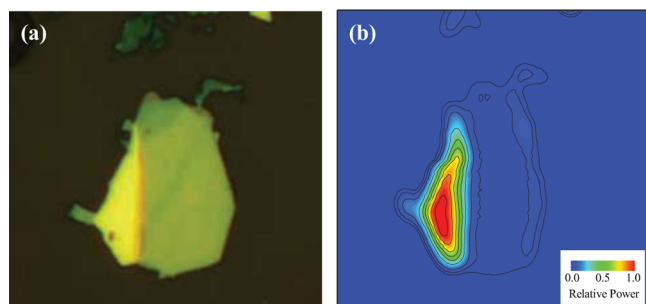
Figure 4. Optical microscopy image (a) and third-harmonic image (b) of a multilayer flake. The length of each side of the images is 25 μm.

flake. The size of the imaged region is 25 by 25 μm^2. According to the contrast in this linear optical image, we can roughly estimate that the flake contains 10−15 atomic layers, with the left side thicker than the right side. The TH image is shown in Figure 4b. The shape of the flake indicated by the THG image is consistent with that shown in the microscopy image. Clearly, several regions with different thicknesses can be easily identified in the TH image, owing to the enhanced contrast.

CONCLUSIONS

In summary, we observed third-harmonic generation in atomically thin layers of MoS_2 and deduced effective third-order nonlinear susceptibilities on the order of 10^{-19} m^2/V^2. By measuring the susceptibility as a function of light wavelength, we found significant enhancement of the susceptibility by the excitonic resonances. We showed that this effect can be used for nonlinear optical identification of MoS_2 atomic layers with higher contrast and higher distinguishing power of multilayer flakes compared to linear optical microscopy. Furthermore, this technique is less restrictive on substrates. Our results suggest the feasibility of exploring other types of third-order nonlinear optical effects for various applications.

AUTHOR INFORMATION

Corresponding Authors
*E-mail: chiu@ku.edu.
*E-mail: huizhao@ku.edu.
Notes
The authors declare no competing financial interest.

ACKNOWLEDGMENTS

REFERENCES

(1) Neto, A. H. C.; Guinea, F.; Peres, N. M. R.; Novoselov, K. S.; Geim, A. K. *Rev. Mod. Phys.* **2009**, *81*, 109−162.
(2) Han, M. T.; Özyilmaz, B.; Zhang, Y. B.; Kim, P. *Phys. Rev. Lett.* **2007**, *98*, 206805.
(3) Li, X.; Wang, X.; Zhang, L.; Lee, S.; Dai, H. *Science* **2008**, *319*, 1229−1232.
(4) Jiao, L.; Zhang, L.; Wang, X.; Diankov, G.; Dai, H. *Nature* **2009**, *458*, 877−880.
(5) Sols, F.; Guinea, F.; Neto, A. H. C. *Phys. Rev. Lett.* **2007**, *99*, 166803.
(6) Zhang, Y.; Tang, T. T.; Girit, C.; Hao, Z.; Martin, M. C.; Zettl, A.; Crommie, M. F.; Shen, Y. R.; Wang, F. *Nature* **2009**, *459*, 820−823.
(7) Xia, F.; Farmer, D. B.; Lin, Y.; Avouris, P. *Nano Lett.* **2010**, *10*, 715−718.
(8) Radisavljevic, B.; Radenovic, A.; Brivio, J.; Giacometti, V.; Kis, A. *Nat. Nanotechnol.* **2011**, *6*, 147−150.
(9) Radisavljevic, B.; Whitwick, M. B.; Kis, A. *ACS Nano* **2011**, *5*, 9934−9938.
(10) Wang, H.; Yu, L. L.; Lee, Y. H.; Shi, Y. M.; Hsu, A.; Chin, M. L.; Li, L. J.; Dubey, M.; Kong, J.; Palacios, T. *Nano Lett.* **2012**, *12*, 4674−4680.
(11) Zhang, Y.; Ye, J.; Matsuhashi, Y.; Iwasa, Y. *Nano Lett.* **2012**, *12*, 1136−1140.
(12) Bertolazzi, S.; Brivio, J.; Kis, A. *ACS Nano* **2011**, *5*, 9703−9709.
(13) He, Q. Y.; Zeng, Z. Y.; Yin, Z. Y.; Li, H.; Wu, S. X.; Huang, X.; Zhang, H. *Small* **2012**, *8*, 2994−2999.
(14) Pu, J.; Yomogida, Y.; Liu, K. K.; Li, L. J.; Iwasa, Y.; Takenobu, T. *Nano Lett.* **2012**, *12*, 4013−4017.
(15) Mak, K. F.; Lee, C.; Hone, J.; Shan, J.; Heinz, T. F. *Phys. Rev. Lett.* **2010**, *105*, 136805.
(16) Splendiani, A.; Sun, L.; Zhang, Y.; Li, T.; Kim, J.; Chim, C. Y.; Galli, G.; Wang, F. *Nano Lett.* **2010**, *10*, 1271−1275.
(17) Gmelin, L. *Gmelin Handbook of Inorganic and Organometallic Chemistry*, 8th ed.; Springer-Verlag: Berlin, 1995; Vol. *B7*.
(18) Kuc, A.; Zibouche, N.; Heine, T. *Phys. Rev. B* **2011**, *83*, 245213.
(19) Yin, Z.; Li, H.; Li, H.; Jiang, L.; Shi, Y.; Sun, Y.; Lu, G.; Zhang, Q.; Chen, X.; Zhang, H. *ACS Nano* **2012**, *6*, 74−80.
(20) Lee, H. S.; Min, S. W.; Chang, Y. G.; Park, M. K.; Nam, T.; Kim, H.; Kim, J. H.; Ryu, S.; Im, S. *Nano Lett.* **2012**, *12*, 3695−3700.
(21) Shanmugam, M.; Bansal, T.; Durcan, C. A.; Yu, B. *Appl. Phys. Lett.* **2012**, *100*, 153901.
(22) Ramasubramaniam, A. *Phys. Rev. B* **2012**, *86*, 115409.
(23) Mak, K. F.; He, K.; Lee, C.; Lee, G. H.; Hone, J.; Heinz, T. F.; Shan, J. *Nat. Mater.* **2013**, *12*, 207−211.
(24) Ross, J. S.; Wu, S.; Yu, H.; Ghimire, N. J.; Jones, A. M.; Aivazian, G.; Yan, J.; Mandrus, D. G.; Xiao, D.; Yao, W.; Xu, X. *Nat. Commun.* **2013**, *4*, 1474.
(25) Cao, T.; Wang, G.; Han, W. P.; Ye, H. Q.; Zhu, C. R.; Shi, J. R.; Niu, Q.; Tan, P. H.; Wang, E.; Liu, B. L.; Feng, J. *Nat. Commun.* **2012**, *3*, 887.
(26) Zeng, H.; Dai, J.; Yao, W.; Xiao, D.; Cui, X. *Nat. Nanotechnol.* **2012**, *7*, 490−493.
(27) Mak, K. F.; He, K.; Shan, J.; Heinz, T. F. *Nat. Nanotechnol.* **2012**, *7*, 494−498.
(28) Xiao, D.; Liu, G. B.; Feng, W.; Xu, X.; Yao, W. *Phys. Rev. Lett.* **2012**, *108*, 196802.
(29) Sallen, G.; Bouet, L.; Marie, X.; Wang, G.; Zhu, C. R.; Han, W. P.; Lu, Y.; Tan, P. H.; Amand, T.; Liu, B. L.; Urbaszek, B. *Phys. Rev. B* **2012**, *86*, 081301.
(30) Gong, Z.; Liu, G.-B.; Yu, H.; Xiao, D.; Cui, X.; Xu, X.; Yao, W. *Nat. Commun.* **2013**, *4*, 2053.
(31) Kumar, N.; Najmaei, S.; Cui, Q.; Ceballos, F.; Ajayan, P. M.; Lou, J.; Zhao, H. *Phys. Rev. B* **2013**, *87*, 161403.
(32) Malard, L. M.; Alencar, T. V.; Barboza, A. P. M.; Mak, K. F.; de Paula, A. M. *Phys. Rev. B* **2013**, *87*, 201401.
(33) Li, Y.; Rao, Y.; Mak, K. F.; You, Y.; Wang, S.; Dean, C. R.; Heinz, T. F. *Nano Lett.* **2013**, *13*, 3329−3333.

(34) Zeng, H.; Liu, G.-B.; Dai, J.; Yan, Y.; Zhu, B.; He, R.; Xie, L.; Xu, S.; Chen, X.; Yao, W.; Cui, X. *Sci. Rep.* **2013**, *3*, 1608.

(35) Sun, Z. P.; Hasan, T.; Torrisi, F.; Popa, D.; Privitera, G.; Wang, F. Q.; Bonaccorso, F.; Basko, D. M.; Ferrari, A. C. *ACS Nano* **2010**, *4*, 803−810.

(36) Hendry, E.; Hale, P. J.; Moger, J.; Savchenko, A. K.; Mikhailov, S. A. *Phys. Rev. Lett.* **2010**, *105*, 097401.

(37) Yang, H. Z.; Feng, X. B.; Wang, Q.; Huang, H.; Chen, W.; Wee, A. T. S.; Ji, W. *Nano Lett.* **2011**, *11*, 2622−2627.

(38) Wu, R.; Zhang, Y. L.; Yan, S. C.; Bian, F.; Wang, W. L.; Bai, X. D.; Lu, X. H.; Zhao, J. M.; Wang, E. G. *Nano Lett.* **2011**, *11*, 5159−5164.

(39) Kumar, N.; Kumar, J.; Gerstenkorn, C.; Wang, R.; Chiu, H. Y.; Smirl, A. L.; Zhao, H. *Phys. Rev. B* **2013**, *87*, 121406.

(40) Hong, S.-Y.; Dadap, J. I.; Petrone, N.; Yeh, P.-C.; Hone, J.; Osgood, R. M. *Phys. Rev. X* **2013**, *3*, 021014.

(41) Zhang, H.; Virally, S.; Bao, Q.; Ping, L. K.; Massar, S.; Godbout, N.; Kockaert, P. *Opt. Lett.* **2012**, *37*, 1856−1858.

(42) Novoselov, K. S.; Jiang, D.; Schedin, F.; Booth, T. J.; Khotkevich, V. V.; Morozov, S. V.; Geim, A. K. *Proc. Natl. Acad. Sci. U.S.A.* **2005**, *102*, 10451−10453.

(43) Benameur, M. M.; Radisavljevic, B.; Héron, J. S.; Sahoo, S.; Berger, H.; Kis, A. *Nanotechnology* **2011**, *22*, 125706.

(44) Castellanos-Gomez, A.; Agraït, N.; Rubio-Bollinger, G. *Appl. Phys. Lett.* **2010**, *96*, 213116.

(45) Boyd, R. W. *Nonlinear Optics*, 3rd ed.; Academy Press: San Diego, CA, 2008.

(46) Wagoner, G. A.; Persans, P. D.; Van Wagenen, E. A.; Korenowski, G. M. *J. Opt. Soc. Am. B* **1998**, *15*, 1017−1021.

(47) Beal, A. R.; Hughes, H. P. *J. Phys. C: Solid State Phys.* **1979**, *12*, 881−890.

(48) Eda, G.; Yamaguchi, H.; Voiry, D.; Fujita, T.; Chen, M.; Chhowalla, M. *Nano Lett.* **2011**, *11*, 5111−5116.

318

dx.doi.org/10.1021/am4042542 | *ACS Appl. Mater. Interfaces* 2014, 6, 314−318